Colloids and Surfaces B: Biointerfaces 94 (2012) 51–57

Contents lists available at SciVerse ScienceDirect

Colloids and Surfaces B: Biointerfaces

journal homepage: www.elsevier.com/locate/colsurfb

# Tocopheryl acetate nanoemulsions stabilized with lipid–polymer hybrid emulsifiers for effective skin delivery

Yoon Sung Nam[a,b,*], Jin-Woong Kim[c,**], JaeYoon Park[b], Jongwon Shim[a,d], Jong Suk Lee[d], Sang Hoon Han[d]

[a] Department of Materials Science and Engineering, Korea Advanced Institute of Science and Technology, 291 Daehak-ro, Yuseong-gu, Daejeon 305-701, Republic of Korea
[b] Department of Biological Sciences, Korea Advanced Institute of Science and Technology, 291 Daehak-ro, Yuseong-gu, Daejeon 305-701, Republic of Korea
[c] Department of Applied Chemistry, Hanyang University, 55 Hanyangdaehak-ro Sangnok-gu, Ansan, Gyeonggi-do 426-791, Republic of Korea
[d] Amore Pacific R&D Center, 314-1 Bora-dong Giheung-gu Yongin-si, Gyeonggi-do 449-729, Republic of Korea

ARTICLE INFO

*Article history:*
Received 1 October 2011
Received in revised form 9 January 2012
Accepted 13 January 2012
Available online 23 January 2012

*Keywords:*
Nanoemulsions
Biodegradable polymers
Polymeric emulsifiers
Phospholipids
Skin drug delivery

ABSTRACT

Tocopheryl acetate is used as the oil component of nanoemulsions using a mixture of unsaturated phospholipids and polyethylene oxide-*block*-poly(ε-caprolactone) (PEO-*b*-PCL). This study investigates the effects of the lipid–polymer composition on the size and surface charge of nanoemulsions, microviscosity of the interfacial layer, and skin absorption of tocopheryl acetate. The lipid–polymer hybrid system exhibits excellent colloidal dispersion stability, which is comparable to that of polymer-based nanoemulsions. If lipids are used as emulsifiers, nanoemulsions show poor dispersion stability despite a good skin absorption enhancing effect. The amount of tocopheryl acetate absorbed by the skin increases with an increased lipid-to-polymer ratio, as determined using the hairless guinea pig skin loaded in a Franz-type diffusion cell. An 8:2 (w/w) mixture of unsaturated phospholipids and PEO-*b*-PCL exhibits the most efficient delivery of tocopheryl acetate into the skin. Our results show that tocopheryl acetate is absorbed almost twice as fast by the lipid–polymer hybrid system than the nanoemulsions stabilized with PEO-*b*-PCL. This study suggests that the lipid–polymer hybrid system can be used as an effective means of optimizing nanoemulsions in terms of dispersion stability and skin delivery capability.



## 1. Introduction

Nanoemulsions have been widely investigated for diverse industrial applications, including pharmaceutical, food, and cosmetic and personal care products, with the aim of enhancing the bioavailability of the encapsulated active compounds by controlling their interactions with biomolecules, cells and tissues [1–7]. The biological effects of nanoemulsions highly depend upon their interfacial properties, which are largely determined by emulsifiers through a combination of multiple interactions, including electrostatic interactions, steric effects, and mechanical forces [8–10]. Accordingly, the choice of appropriate emulsifiers is critically important in controlling the functional properties of nanoemulsions, including physical stability and interactions with biological systems [1,11,12].

Lipids and fatty acids have been commonly used as emulsifiers to stabilize nanoemulsions because of their well-known biocompatibility and a wide spectrum of amphiphilic molecular structures [6,13–15]. However, despite the good performances in interfacial stabilization, small molecular weight emulsifiers are very dynamic at the interfaces, easily allowing the fusion and fission of emulsions [16,17]. Accordingly, the emulsions prepared with lipid emulsifiers are susceptible to thermal and mechanical stresses, limiting their practical applications [18]. Because of these limitations, polymeric amphiphiles have been considered as alternative emulsifiers [19,20]. In contrast to low molecular weight counterparts, polymeric emulsifiers can form a mechanically robust film at the interface, which can contribute to the effective stabilization of nanoemulsions. Such structural robustness of polymeric systems is beneficial in maintaining the physical structures of nanoemulsions. However, some degree of structural flexibility of delivery carriers is often required for the controlled release of encapsulated ingredients and the efficient transport of active molecules into biological systems. For instance, lipid emulsifiers have been shown to effectively facilitate the transdermal transport of hydrophobic molecules through the disturbance of the lipid-rich domain, which is known as a translocation route for hydrophobic molecules in the skin [21–25]. Therefore, lipids and

* Corresponding author at: Department of Materials Science and Engineering, Korea Advanced Institute of Science and Technology, 291 Daehak-ro, Yuseong-gu, Daejeon 305-701, Republic of Korea.
** Corresponding author.
*E-mail addresses:* yoonsung@kaist.ac.kr (Y.S. Nam), kjwoong@hanyang.ac.kr (J.-W. Kim).

0927-7765/$ – see front matter © 2012 Elsevier B.V. All rights reserved.
doi:10.1016/j.colsurfb.2012.01.016

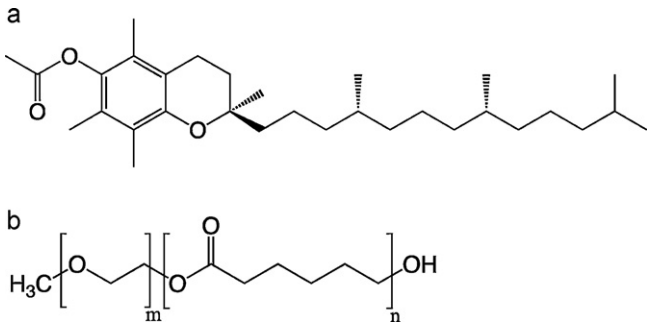


**Fig. 1.** Chemical structures of (a) tocopheryl acetate (TA) and (b) $PEO_{45}$-*b*-$PCL_{42}$ ($m = 45$ and $n = 42$).

polymers seem to have their own unique benefits as emulsifiers for nanoemulsions.

In this study, we investigated the combination of lipids and polymers as a facile method to optimize the physicochemical properties of nanoemulsions as skin absorption carriers. Various mixture compositions of unsaturated phospholipids and amphiphilic polymers were used to prepare oil-in-water (O/W) nanoemulsions incorporating tocopheryl acetate (TA) as the oil phase. TA is a prodrug compound of α-tocopherol, which is the most prominent, naturally occurring form of vitamin E (Fig. 1a). Tocopherol and its derivatives are antioxidant oils widely used for dermatological or personal care products because of their well-known biological activities, including photo-protective actions in the skin [26–29]. A di-block copolymer, poly(ethylene oxide)-*block*-poly(ε-caprolactone) (PEO-*b*-PCL, Fig. 1b), was used as a co-emulsifier with unsaturated phospholipids. Our recent studies showed that PEO-*b*-PCL effectively reinforces the emulsion interface through the formation of a mechanically stable semi-solid film that can resist the coarsening processes of emulsions [30,31]. PCL is a good hydrophobic block segment for this purpose because of its relatively low melting temperature ($T_m$ = 50–60 °C). Above $T_m$, PEO-*b*-PCL is readily miscible with phospholipids. The effects of the composition of the polymer–lipid mixture on the size, surface charge, microviscosity and dispersion stability of the prepared TA nanoemulsions were studied.

## 2. Experimental

### 2.1. Materials

Methoxy PEO (mPEO, average molecular weight = 2 kDa), ε-caprolactone, stannous octoate ($Sn(Oct)_2$), ethylenediaminetetraacetic acid (EDTA), 1,6-diphenyl-1,3,5-hexatriene (DPH), and tetramethylsilane were purchased from Sigma–Aldrich (St. Louis, MO, USA). Hydrogenated soybean lecithin (Lipoid S75-3, 70–75% phosphatidylcholine) and phospholipon 90G (P90G, mostly soybean phosphatidylcholine with *max.* 4.0% lysophosphatidylcholine) were obtained from Lipoid GmbH (Ludwigshafen, Germany) and Phospholipid GmbH (Cologne, Germany), respectively. Female hairless guinea pigs (strain IAF/HA-hrBR, 6–8 weeks old) were obtained from Charles River Laboratories (Willmington, MA, USA).

### 2.2. Synthesis and characterization of PEO-b-PCL

PEO-*b*-PCL diblock copolymer was synthesized by ring opening polymerization of ε-caprolactone with mPEO as an initiator. A known amount of ε-caprolactone was introduced into a silanized round-bottom Erlenmeyer flask containing a pre-weighed amount of mPEO and $Sn(Oct)_2$. The flask was connected to a vacuum line, evacuated, sealed off and placed at 120 °C. After 24 h the resulting block copolymers were dissolved in methylene chloride and precipitated in excess cold methanol. Polymers were dried under vacuum for 2 days. The copolymers were characterized by gel permeation chromatography (GPC). A high performance liquid chromatography (HPLC) system composed of Agilent 110 series (Agilent Technologies, Palo Alto, CA, USA) and a refractive index detector was operated by using a series of three PLgel columns (300 mm × 7.5 mm, pore size = 103, 104, and 105 Å) as a size exclusion column; tetrahydrofuran as an isocratic mobile phase; 1.0 mL $min^{-1}$ as a flow rate; monodisperse polystyrene samples as calibration standards. $^1H$ Nuclear magnetic resonance (NMR) spectra were taken at 25 °C with a Gemini-300BB NMR operating at 300.06 MHz using a solvent, $CDCl_3$, and chemical shifts were measured in parts per million using tetramethylsilane as an internal reference.

### 2.3. Preparation of nanoemulsions

One and a half grams of emulsifiers (P90G, S75-3, PEO-*b*-PCL, or their mixtures) were dissolved in a 1:1 mixture of propylene glycol and absolute ethanol (10 g) at 70 °C. Five grams of TA were mixed with the solution, and then this organic solution was then poured into pre-heated Milli-Q water (83.5 g). The mixture was emulsified at 5000 rpm for 3 min using a T. K. homo-mixer Mark II f model (Tokushu Kika Co. Ltd, Osaka, Japan). The coarse emulsions were then pumped through an interaction chamber of a M110EH microfluidizer (Microfluidics Corp., Newton, MA, USA) at the maximum pulse pressure of about 1000 bar. The nanoemulsions were cooled to ambient temperature during the microfluidic homogenization as the temperature of the interaction chamber and channels was maintained around 15 °C by a circulating water jacket. A schematic diagram of the microfluidic system used in this work is provided in our previous report [32].

### 2.4. Characterization

To observe the morphology of nanoemulsions, a drop of the sample with a concentration of 50 mg $mL^{-1}$ was placed onto a 100 mesh copper grid coated with carbon (Ted Pella). After deposition, the grid was tapped with a filter paper to remove surface water and negatively stained using 1% uranyl acetate. The samples were then dried in air at ambient temperature. Transmission electron micrographs of nanoemulsions were taken on a JEOL 1010 electron microscope (Akishima, Japan) operated at 200 kV. Differential scanning calorimetry (DSC) analysis was carried out using a TA2010 thermal analyzer instrument (TA instruments, New Castle, DE). A heating scan was performed at a rate of 10 °C $min^{-1}$ from 10 to 160 °C. Size distribution and zeta potential were measured by dynamic laser light scattering (DLS) technique with a He/Ne laser of 633 nm (Zetasizer 3000HS, Malvern, UK). The scattering angle was fixed at 90°, and the temperature was maintained at 25 °C. The experimental correlation function was measured, and the hydrodynamic diameter was calculated by the Contin method, which gives access to the distribution of relaxation times in the experimental time correlation functions. The electrophoretic mobility was measured with a laser Doppler velocimetry, where the velocity of moving particles is determined by Doppler frequency shifts of scattered laser light. A capillary cell was used with an applied electric voltage of 29 V $cm^{-1}$ at 25 °C. In order to exclude the electroosmotic effect, the fast field reversal method was used, that is, the frequency was set at 50 Hz. Zeta potential ($\zeta$) was calculated from the electrophoretic mobility ($\mu$) by the Helmholtz–Smoluchowski approximation: $\zeta = \mu \cdot \eta \cdot D^{-1} \cdot \varepsilon_0{}^{-1}$, where $\mu$ is the electrophoretic mobility, $D$ is the dielectric constant of water (78.54 at 25 °C), and $\varepsilon_0$ is the vacuum permittivity ($8.854 \times 10^{-12}$ F $m^{-1}$). In order to measure the anisotropy of hydrophobic domain, 2 mL of 2 mM DPH in

tetrahydrofuran was added to 2 mL of the sample (1 mg mL$^{-1}$). The samples with DPH were mixed by vortex vigorously to facilitate the partition of DPH into the organic phase. The steady-state emission anisotropy ($r$) of DPH was defined as the following equation: $r = (I_0 - I_{90})/(I_0 + 2I_{90})$, where $I_0$ and $I_{90}$ are the components of the emission intensity polarized parallel and perpendicular to the electric vector of the plane-polarized excitation, respectively. Emission intensities were recorded on a Hitachi F-4500 spectrophotometer (Nissei Sangyo Co. Ltd, Tokyo, Japan). The excitation wavelength was set at 360 nm, and the emission was measured at 430 nm with 400 V of the photomultiplier voltage, and excitation and emission slit widths of 2.5 mm and 5.0 mm, respectively. Colloidal stability of nanoemulsions was measured using a two-point conductivity method with a DualCon stability tester (ITEC-IFAC Technology GmbH & Co. KG, Duisburg, Germany). Two pairs of electrodes determined the conductivity at the top ($\kappa_1$) and at the bottom ($\kappa_2$) of the sample placed in a cylindrical container. The conductivity difference ($\Delta\kappa = \kappa_2 - \kappa_1$) was used to determine the colloidal stability of nanoemulsion samples.

### 2.5. In vitro skin absorption analysis

*In vitro* skin absorption of TA in different nanoemulsions was carried out using a Franz-type diffusion cell (Model FCDS-1200C, Fine Scientific, Korea). Female hairless guinea pigs were used since they have a relatively thick epidermis that does not require shaving. The abdominal skin was excised and divided to mount on the diffusion cells (0.9 cm in diameter). The receptor compartment (5 mL) was filled with 50 mM phosphate buffered saline (PBS, pH 7.0, 20 mM NaCl) with magnetic stirring at 200 rpm. Nanoemulsions (0.5 mL) containing 5 wt% TA were carefully applied to the skin surface in the donor compartment, and the temperature was maintained at 32 °C using a circulating water jacket. At predetermined time intervals the skin samples were rinsed with 5 mL PBS three times. After the skin was separated from the diffusion cell, it was fixed on a clean, flat rubber sheet and dried in air at ambient temperature for 1 h in the dark. The stratum corneum of the dried skin specimens was removed by taping the skin surface with a 3 M Magic tape five times. The skin was then ground in methanol using a pulverizer (Polytron PT2100. Switzerland) to extract TA from the skin, and then the extract was filtered through a 0.45 μm nylon membrane. The amount of TA was analyzed with a $C_{18}$ reversed-phase column (Nova-Pak® $C_{18}$, 3.9 mm × 150 mm, Waters) by a HPLC system composed of Agilent 1100 series. The flow rate of the eluents was fixed at 0.8 mL min$^{-1}$. The mobile phase was a 95/5 (v/v) mixture of methanol and deionized distilled water, and the eluate was monitored by UV absorption measurement at 208 nm.

## 3. Results and discussion

PEO-*b*-PCL was synthesized through the ring opening polymerization of ε-caprolactone with mPEO as an initiator. The weight average molecular weight and the polydispersity were 7.3 kDa and 1.37, respectively, as determined by GPC. The measured molar ratio of PCL to PEO was 1.07:1 as determined by $^1$H NMR spectroscopy, and thus the synthesized block copolymer was denoted as $PEO_{45}$-*b*-$PCL_{42}$. At ambient temperature, $PEO_{45}$-*b*-$PCL_{42}$ was not dissolved in TA in the tested concentration range of 0.5–5 wt%. However, when $PEO_{45}$-*b*-$PCL_{42}$ was dissolved in a 1:1 (w/w) mixture of propylene glycol and ethanol, the block copolymer solution was miscible with TA, resulting in transparent solution at 70 °C. Nanoemulsions were prepared by dispersing the organic solution containing TA and emulsifiers (P90G, $PEO_{45}$-*b*-$PCL_{42}$, or their mixtures) into Milli-Q water at 70 °C under homogenization at 5000 rpm to produce micron-sized emulsions. The embryonic emulsions were pumped through a microchannel, referred to as an interaction chamber, of a M110EH microfluidizer at the maximum pulse pressure of about 1000 bar, producing nano-sized emulsions [32]. The nanoemulsion structure was frozen immediately after the microfluidic homogenization as the temperature of the interaction chamber and channels was maintained around 15 °C using a circulating cold water jacket.

Fig. 2 shows the TEM images of the prepared nanoemulsions incorporating TA as an oil component. The nanoemulsions stabilized by P90G, mostly comprising unsaturated phospholipids, showed a low image contrast despite negative staining with 1% uranyl acetate, and their average diameter was in the range of 60–80 nm in diameter with a relatively uniform size distribution. A DLS analysis showed that the nanoemulsions have a unimodal size distribution with a mean hydrodynamic diameter of 100.2 ± 2.8 nm (Fig. 3). This value is approximately 50% larger than the emulsion size estimated from the TEM image, indicating that the severe shrinkage of the nanoemulsions occurred during the sample drying on a TEM grid. The low image contrast might be affected by the oil absorption to the grid because some emulsions, particularly large ones, could be collapsed, and the oils were then easily absorbed by the grid coated with a carbon film having a strong affinity to hydrophobic molecules. By contrast, the mean diameter of the nanoemulsions stabilized by $PEO_{45}$-*b*-$PCL_{42}$ was 146.9 ± 1.5 nm (Figs. 2b and 3), which was consistent between the TEM and DLS analyses. This result indicates that the interfacial layer formed by the polymeric emulsifier avoided severe structural changes during the drying process for TEM analysis. It is reasonable because the semi-crystalline PCL block of $PEO_{45}$-*b*-$PCL_{42}$ is solidified at the emulsion interface at ambient temperature.

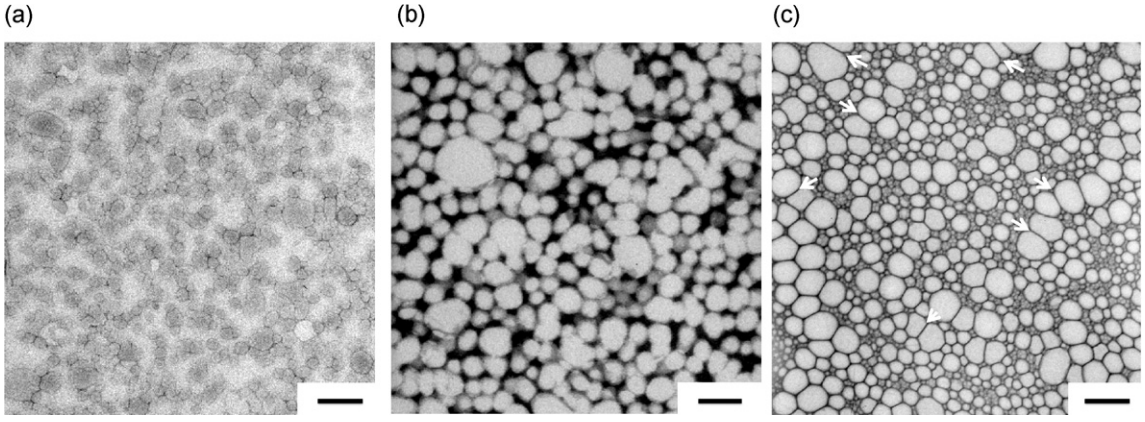


**Fig. 2.** Transmission electron micrographs of the TA nanoemulsions prepared using (a) P90G, (b) $PEO_{45}$-*b*-$PCL_{42}$, and (c) a 1:1 mixture of P90G and $PEO_{45}$-*b*-$PCL_{42}$. The images were taken from the samples negatively stained with 1% uranyl acetate. The scale bars = 150 nm.

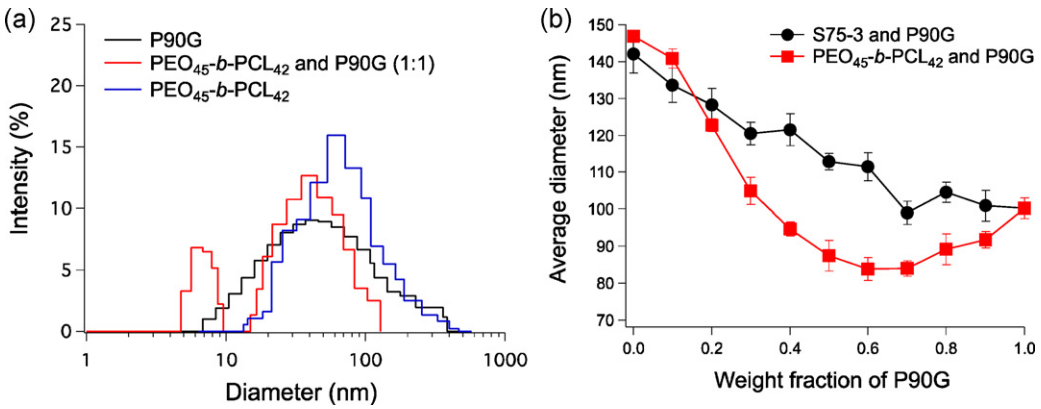


**Fig. 3.** (a) The size distribution of TA nanoemulsions prepared through high-pressure microfluidization at 1000 bar. (b) The average hydrodynamic diameters of TA nanoemulsions as a function of the weight fraction of 90G. The nanoemulsions were stabilized with P90G mixed with $PEO_{45}$-*b*-$PCL_{42}$ or S75-3. The error bars indicate the standard deviation of >10 measurements.

The melting temperature of the block copolymer was around 57.5 °C, as measured by DSC (Fig. 4). The nanoemulsions stabilized with a 1:1 mixture of P90G and $PEO_{45}$-*b*-$PCL_{42}$ had a bi-modal size distribution, which was also consistent with the TEM image (Fig. 2c). The larger emulsions exhibited apparent deformation, as indicated with arrows in the image, due to the close packing of the nanoemulsions during the drying process. This deformation illustrated that the interfacial layer formed by a mixture of P90G and $PEO_{45}$-*b*-$PCL_{42}$ is semi-solid and more flexible compared to the $PEO_{45}$-*b*-$PCL_{42}$ layer. The bi-modal size distribution implied the possibility that lipids were macroscopically separated from polymers during the emulsification. However, the DSC results indicated that the melting temperature of $PEO_{45}$-*b*-$PCL_{42}$ was completely shifted from 57.5 °C to 51.0 °C when it was mixed with P90G at the 1:1 weight ratio (Fig. 4). This result indicated that the two materials were homogeneously mixed, or blended, at the molecular level rather than a macroscopic phase separation.

We further investigated the effects of the composition of P90G and $PEO_{45}$-*b*-$PCL_{42}$ on the size distribution, surface potential, and microviscosity of the prepared nanoemulsions. A mixture of P90G and S75-3 (hydrogenated phospholipids) was also used as an emulsifier for comparison in order to clarify the role of $PEO_{45}$-*b*-$PCL_{42}$. In the case of the mixed lipid emulsifier, the hydrodynamic diameter of nanoemulsions gradually increased with the increased weight fraction of S75-3 (Fig. 3b). This finding can be explained by the formation of the liquid crystalline lamellar structure of the saturated lipids in S75-3 at ambient temperature. The lipid lamellar phase can decrease the curvature of the interfacial layer of the nanoemulsions and contribute to the size increase of nanoemulsions [33]. When the nanoemulsions were stabilized with a mixture of P90G and $PEO_{45}$-*b*-$PCL_{42}$, the nanoemulsions have the smallest size at the 6:4 (w/w) ratio of P90G and $PEO_{45}$-*b*-$PCL_{42}$, indicating the most effective molecular packing of the emulsifiers at the interface (Fig. 3b). In addition, the negative surface potential increased with the increased amount of S75-3 (Fig. 5a). This negative surface charge seems to be induced by fatty acids in S75-3 and might contribute to the electrostatic stabilization of the nanoemulsions. The surface potential of the nanoemulsions stabilized by the mixture of P90G and $PEO_{45}$-*b*-$PCL_{42}$ slightly increased with increasing the amount of $PEO_{45}$-*b*-$PCL_{42}$. This result indicates that the colloidal stabilization by $PEO_{45}$-*b*-$PCL_{42}$ was mostly ascribed to the steric hindrance effects of the PEO chain rather than electrostatic interactions. Fig. 5b shows that the fluorescence anisotropy of DPH decreased with the increased weight fraction of P90G regardless of its use with S75-3 or $PEO_{45}$-*b*-$PCL_{42}$. Both of the crystalline molecules, regardless of the molecular size and structure, increased the microviscosity of the interfacial layer. However, the anisotropy of the nanoemulsions stabilized with the mixed lipids gradually decreased with the increasing fraction of P90G, while the mixture of $PEO_{45}$-*b*-$PCL_{42}$ and P90G exhibited the slight decrease of the anisotropy up to 70 wt% of P90G, followed by the abrupt reduction at 80 wt%. These results imply different interfacial structures between lipid emulsifiers and polymer–lipid mixtures at the molecular level.

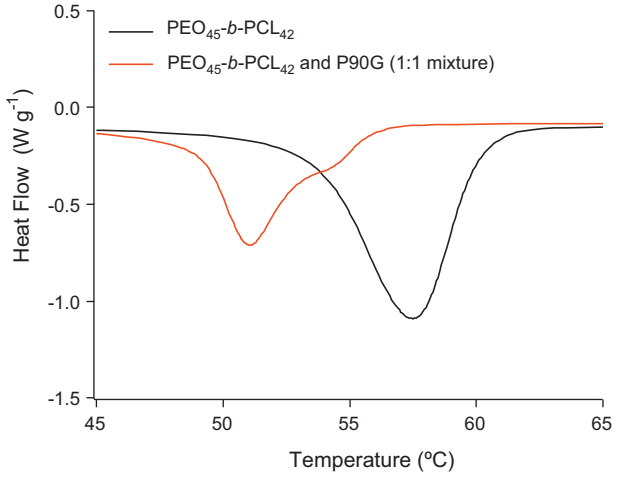


**Fig. 4.** DSC diagrams of $PEO_{45}$-*b*-$PCL_{42}$ (black) and a 1:1 mixture of $PEO_{45}$-*b*-$PCL_{42}$ and P90G (red). (For interpretation of the references to color in this figure legend, the reader is referred to the web version of the article.)

The colloidal dispersion stability of the nanoemulsions was examined using the two-point conductivity method. This method is based on the variation of the electrochemical potential ($\Delta\kappa$), which is defined as the difference between the ion conductivities at the top ($\kappa_1$) and bottom ($\kappa_2$) of an emulsion sample [30]. The conductivity analysis is very sensitive to the variations of local phase fluctuations of emulsions, which cause the change in chemical compositions, so that an apparent change of $\Delta\kappa$ can be quickly detected even in the case of no obvious phase separation. Fig. 6a compares the temporal changes of the electrochemical potential of different nanoemulsion formulations monitored at 50 °C. The phase fluctuation of the nanoemulsions was the largest in the P90G nanoemulsions, while the $PEO_{45}$-*b*-$PCL_{42}$ nanoemulsions showed the smallest temporal variation: the average potential values were $\Delta\kappa = 56.7 \pm 1.9\ \mu S\ cm^{-1}$ for P90G and $\Delta\kappa = 17.8 \pm 1.1\ \mu S\ cm^{-1}$ for $PEO_{45}$-*b*-$PCL_{42}$, respectively. Interestingly, the nanoemulsions stabilized by the 1:1 mixture of $PEO_{45}$-*b*-$PCL_{42}$ and P90G showed the intermediate level of $\Delta\kappa = 28.2 \pm 0.8\ \mu S\ cm^{-1}$, which was about 50%

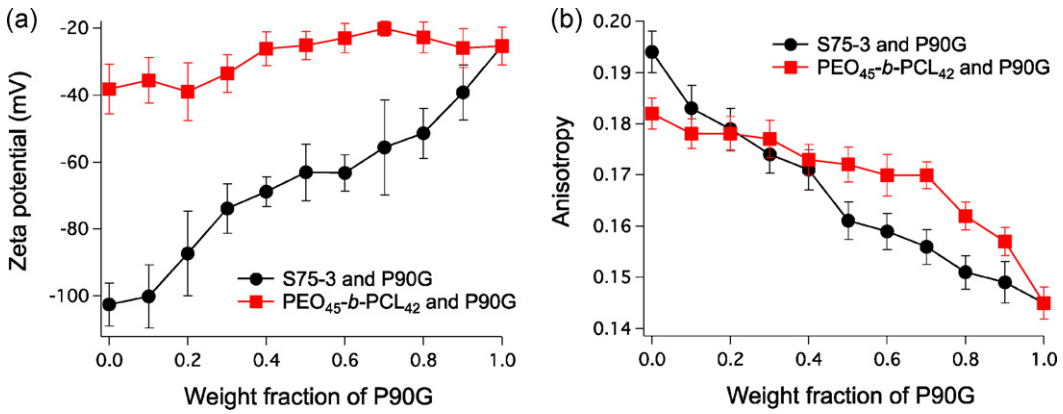


**Fig. 5.** Zeta potential (a) and DPH anisotropy (b) of TA nanoemulsions as a function of the weight fraction of P90G. The nanoemulsions were stabilized with P90G mixed with $PEO_{45}$-*b*-$PCL_{42}$ or S75-3. The error bars indicate the standard deviation of 6–8 measurements for zeta potential and 5 measurements for DPH anisotropy.

of the value for P90G. Although the combination of P90G and $PEO_{45}$-*b*-$PCL_{42}$ increased the dispersion stability for a short period of time, it was not certain whether the nanoemulsions would practically maintain the dispersion stability for an extended period of time. In order to examine the long-term physical integrity, the size distribution of the nanoemulsions was determined after the incubation at 50 °C for 30 days. The average diameter of the P90G nanoemulsions increased from 100.2 ± 2.8 nm to 165.7 ± 3.9 nm, while the $PEO_{45}$-*b*-$PCL_{42}$ nanoemulsions showed almost the same average emulsion size: 146.9 ± 1.5 nm at 1 h after preparation and 149.1 ± 2.3 nm on 30 days after incubation at 50 °C. Fig. 6b shows that the nanoemulsions stabilized by the 1:1 mixture of $PEO_{45}$-*b*-$PCL_{42}$ and P90G also had no significant changes in the size distribution after the 30-day incubation at 50 °C. The average diameters were 87.4 ± 4.1 nm at 1 h after preparation and 91.9 ± 4.3 nm on 30 days after incubation at 50 °C. These results demonstrated that the combination of unsaturated lipids and amphiphilic polymers could be an effective means of maintaining the dispersion stability of nanoemulsions as well as producing the smaller size of nanoemulsions.

Tocopherol is a powerful antioxidant that can protect the skin against UV light-induced biological damages [26–29]. Although TA is a prodrug conjugate of tocopherol and acetate, it can be hydrolyzed to biologically active D-alpha-tocopherol through enzymatic cleavage in the skin [34]. To investigate the *in vitro* skin absorption of TA from different nanoemulsion formulations, the abdominal skin of female hairless guinea pigs was used because it has a relatively thick epidermis and does not require shaving [35,36]. The excised skin was mounted on a Franz-type diffusion cell, and a nanoemulsion sample was carefully applied to the skin surface. At the predetermined intervals the sample was removed from the diffusion cell, rinsed with PBS, and pulverized using a homogenizer to extract TA from the skin. All of the prepared nanoemulsions were used for skin absorption studies within one day after the preparation in order to exclude the possibility that any structural changes or colloidal instability were involved in the skin absorption process. Fig. 7a shows the cumulative profiles of the *in vitro* skin absorption of TA from the nanoemulsions prepared using a mixture of P90G and $PEO_{45}$-*b*-$PCL_{42}$ at various mixing ratios. Interestingly, when the weight fraction of P90G is below 40 wt%, the amount of TA absorbed by the skin was practically independent of the composition of the emulsifiers. Above 40 wt% of P90G, the skin absorption of TA increased with the increased weight fraction of P90G up to 80 wt%. Since the size of nanoemulsions was relatively small at 80 wt% of P90G, it was examined whether the size of the nanoemulsions is a major determining factor for the skin absorption of TA. To this end, the same block copolymer with a shorter PCL chain, $PEO_{45}$-*b*-$PCL_{25}$ (MW 5.4 kDa), was synthesized and used to prepare smaller TA nanoemulsions.

The measured hydrodynamic diameters of the nanoemulsions stabilized with $PEO_{45}$-*b*-$PCL_{25}$ and $PEO_{45}$-*b*-$PCL_{42}$ were 108.0 ± 2.9 nm and 146.9 ± 1.5 nm, respectively. The zeta potentials ($\zeta$) of the nanoemulsions were similar: $\zeta = -41.2 \pm 6.7$ mV for $PEO_{45}$-*b*-$PCL_{25}$ and $\zeta = -38.2 \pm 7.3$ mV for $PEO_{45}$-*b*-$PCL_{42}$. The amounts of TA absorbed by the skin for 24 h were also very similar between the two polymer-based nanoemulsions: 18.9 ± 1.6 μg $cm^{-2}$ from $PEO_{45}$-*b*-$PCL_{42}$ (A, Fig. 7b) and

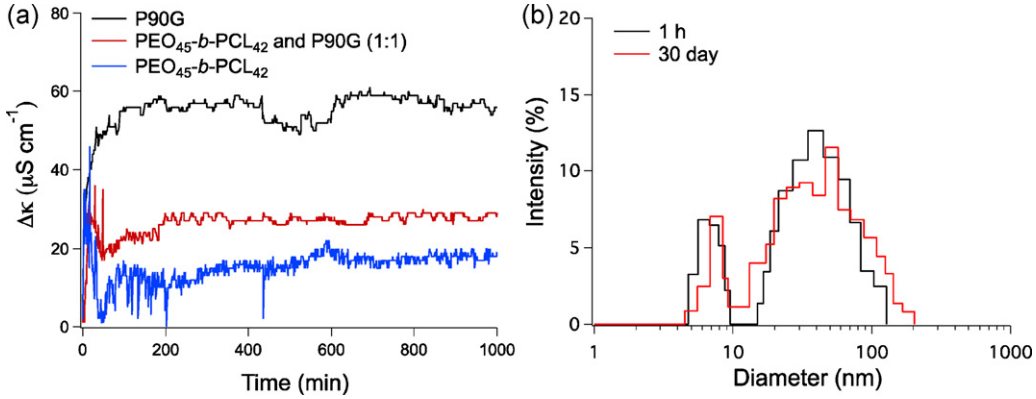


**Fig. 6.** (a) Temporal variations of the electrochemical potentials of the nanoemulsions measured at 50 °C. (b) Size distribution of the nanoemulsions stabilized by the 1:1 mixture of $PEO_{45}$-*b*-$PCL_{42}$ and P90G at 1 h after preparation (black) and on 30 day after incubation at 50 °C (red). (For interpretation of the references to color in this figure legend, the reader is referred to the web version of the article.)

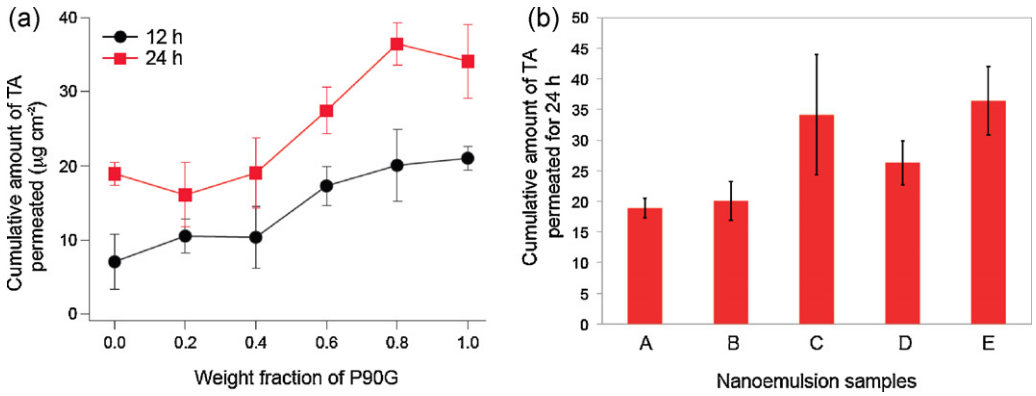


**Fig. 7.** Cumulative amount of TA absorbed by the hairless guinea pig skin from nanoemulsions. (a) The cumulative amount of TA absorbed from the nanoemulsions stabilized using a mixture of P90G and $PEO_{45}$-*b*-$PCL_{42}$ as a function of the lipid–polymer ratio for 12 h (black) and 24 h (red). (b) The cumulative amount of TA absorbed for 24 h from various TA nanoemulsions stabilized using $PEO_{45}$-b-$PCL_{42}$ (A), $PEO_{45}$-b-$PCL_{25}$ (B), 90G (C), and an 8:2 mixture of 90G and $PEO_{45}$-b-$PCL_{42}$ (D), and 90G and $PEO_{45}$-b-$PCL_{25}$ (E). Each point represents the mean ± standard deviation of 3–5 experiments. (For interpretation of the references to color in this figure legend, the reader is referred to the web version of the article.)

$20.1 \pm 3.2\ \mu g\,cm^{-2}$ from $PEO_{45}$-*b*-$PCL_{25}$, respectively (B, Fig. 7b). In addition, the amount of TA absorbed from $PEO_{45}$-*b*-$PCL_{25}$ was only 58.9% of that from the lipid-based nanoemulsions ($34.1 \pm 4.9\ \mu g\,cm^{-2}$ from P90G, C, Fig. 7b) despite the similar emulsion sizes: $108.0 \pm 2.9$ nm for $PEO_{45}$-*b*-$PCL_{25}$ and $100.2 \pm 2.8$ nm for P90G. These results indicated that the enhanced trans-epidermal delivery of TA from nanoemulsions is not simply determined by the size of nanoemulsions, but the incorporation of the unsaturated phospholipids into the nanoemulsions is essential to facilitate the skin absorption of TA. It is worth noting that unsaturated lipids and fatty acids could be skin permeation enhancers because they can reorganize the lipid structures in the skin. In our previous report, the skin absorption enhancing effect of P90G was demonstrated using caffeine as an active molecule loaded into liposomes [22]. In order to further clarify the impact of the size of nanoemulsions on the skin absorption of TA, the size of nanoemulsions with the same chemical composition was adjusted by changing the applied pressure in the microfluidic process. The weight ratio of P90G and $PEO_{45}$-*b*-$PCL_{42}$ was fixed at 8:2. The average diameters of the prepared nanoemulsions were $183.4 \pm 2.9$ nm and $89.2 \pm 4.1$ nm at the applied pressure of 500 bar and 1000 bar, respectively. The size of the lipid–polymer hybrid nanoemulsions having the same chemical composition significantly affected the TA absorption into the skin: $26.3 \pm 3.6\ \mu g\,cm^{-1}$ from the larger nanoemulsions (D, Fig. 7b) and $36.4 \pm 5.6\ \mu g\,cm^{-1}$ from the smaller ones (E, Fig. 7b). This result indicates that both of the size and chemical composition need to be simultaneously considered for effective skin delivery of TA.

## 4. Conclusions

This study has demonstrated that the combination of unsaturated phospholipids and amphiphilic block copolymers can be an effective means of enhancing the skin delivery capability of nanoemulsions while maintaining the long-term dispersion stability. In particular, in the range of the 5:5–2:8 weight ratios of PEO-*b*-PCL to unsaturated phospholipids, large variations were found in the emulsion size, microviscosity, and the skin absorption efficiency. The interesting aspect of our study is that the emulsifier having a skin absorption enhancing activity can be co-localized with biological active ingredients into a nano-carrier. We expect that this co-encapsulation approach is potentially useful for a selective skin permeation activity. To maximize the effectiveness of nanoemulsion formulations, our study suggests that it is important to carefully optimize the flexibility and robustness of the nanostructures, both of which are critically important for the efficient delivery capability and physical stability of nanoemulsions. In particular, both of the chemical properties (*e.g.*, compositions) and physical parameters (*e.g.*, size) need to be considered to understand the impact of nanoscale materials on biological effects (*e.g.*, skin absorption).

## Acknowledgments

We thank Dr. Young-Jin Lee and Dr. Seung Jae Baik for helpful discussion. This work was supported by the research fund of Hanyang University (HY-2011-N) and Amore Pacific Corporation (Seoul, Republic of Korea).

## References

[1] V. Bali, M. Ali, J. Ali, Study of surfactant combinations and development of a novel nanoemulsion for minimising variations in bioavailability of ezetimibe, Colloids Surf. B Biointerf. 76 (2010) 410–420.
[2] F. Shakeel, W. Ramadan, Transdermal delivery of anticancer drug caffeine from water-in-oil nanoemulsions, Colloids Surf. B Biointerf. 75 (2010) 356–362.
[3] P.E. Makidon, A.U. Bielinska, S.S. Nigavekar, K.W. Janczak, J. Knowlton, A.J. Scott, N. Mank, Z. Cao, S. Rathinavelu, M.R. Beer, J.E. Wilkinson, L.P. Blanco, J.J. Landers, J.R. Baker Jr., Pre-clinical evaluation of a novel nanoemulsion-based hepatitis B mucosal vaccine, PLoS ONE 3 (2008) e2954.
[4] J.M. Janjic, M. Srinivas, D.K. Kadayakkara, E.T. Ahrens, Self-delivering nanoemulsions for dual fluorine-19 MRI and fluorescence detection, J. Am. Chem. Soc. 130 (2008) 2832–2841.
[5] S. Khandavilli, R. Panchagnula, Nanoemulsions as versatile formulations for paclitaxel delivery: peroral and dermal delivery studies in rats, J. Invest. Dermatol. 127 (2007) 154–162.
[6] S. Liu, C.M. Lee, S. Wang, D.R. Lu, A new bioimaging carrier for fluorescent quantum dots: phospholipid nanoemulsion mimicking natural lipoprotein core, Drug Deliv. 13 (2006) 159–164.
[7] E. Yilmaz, H.H. Borchert, Effect of lipid-containing, positively charged nanoemulsions on skin hydration, elasticity and erythema – an in vivo study, Int. J. Pharm. 307 (2006) 232–238.
[8] S.I. Karakashev, E.D. Manev, R. Tsekov, A.V. Nguyen, Effect of ionic surfactants on drainage and equilibrium thickness of emulsion films, J. Colloid Interface Sci. 318 (2008) 358–364.
[9] K.D. Danov, T.D. Gurkov, T. Dimitrova, I.B. Ivanov, D. Smith, Hydrodynamic theory for spontaneously growing dimple in emulsion films with surfactant mass transfer, J. Colloid Interface Sci. 188 (1997) 313–324.
[10] C. Stenvot, D. Langevin, Study of viscoelasticity of soluble monolayers using analysis of propagation of excited capillary waves, Langmuir 4 (1988) 1179–1183.
[11] L. Dai, W. Li, X. Hou, Effect of the molecular structure of mixed nonionic surfactants on the temperature of miniemulsion formation, Colloids Surf. A Physicochem. Eng. Aspects 125 (1997) 27–32.
[12] L. Wang, R. Tabor, J. Eastoe, X. Li, R.K. Heenan, J. Dong, Formation and stability of nanoemulsions with mixed ionic-nonionic surfactants, Phys. Chem. Chem. Phys. 11 (2009) 9772–9778.
[13] R.S. Teixeira, C.J. Valduga, L.A. Benvenutti, S. Schreier, R.C. Maranhao, Delivery of daunorubicin to cancer cells with decreased toxicity by association with a lipidic nanoemulsion that binds to LDL receptors, J. Pharm. Pharmacol. 60 (2008) 1287–1295.

[14] K.K. Singh, S.K. Vingkar, Formulation, antimalarial activity and biodistribution of oral lipid nanoemulsion of primaquine, Int. J. Pharm. 347 (2008) 136–143.
[15] H. Ichikawa, T. Watanabe, H. Tokumitsu, Y. Fukumori, Formulation considerations of gadolinium lipid nanoemulsion for intravenous delivery to tumors in neutron-capture therapy, Curr. Drug Deliv. 4 (2007) 131–140.
[16] T. Yamaguchi, K. Nishizaki, S. Itai, H. Hayashi, H. Ohshima, Physicochemical characterization of parenteral lipid emulsion: influence of cosurfactants on flocculation and coalescence, Pharm. Res. 12 (1995) 1273–1278.
[17] L. Wang, X. Li, G. Zhang, J. Dong, J. Eastoe, Oil-in-water nanoemulsions for pesticide formulations, J. Colloid Interface Sci. 314 (2007) 230–235.
[18] T. Tadros, R. Izquierdo, J. Esquena, C. Solans, Formation and stability of nanoemulsions, Adv. Colloid Interface Sci. 108–109 (2004) 303–318.
[19] T.J. Barnes, I. Ametov, C.A. Prestidge, Naphthalene sulfonate functionalized dendrimers at the solid–liquid interface: influence of core type, ionic strength, and competitive ionic adsorbates, Langmuir 24 (2008) 12398–12404.
[20] C. Solans, P. Izquierdo, J. Nolla, N. Azemar, M.J. Garcia-Celma, Nano-emulsions, Curr. Opin. Colloid Interface Sci. 10 (2005) 102–110.
[21] G. Cevc, G. Blume, Lipid vesicles penetrate into intact skin owing to the transdermal osmotic gradients and hydration force, Biochim. Biophys. Acta 1104 (1992) 226–232.
[22] C. Kim, J. Shim, S. Han, I. Chang, The skin-permeation-enhancing effect of phosphatidylcholine: caffeine as a model active ingredient, J. Cosmet. Sci. 53 (2002) 363–374.
[23] Y. Yokomizo, H. Sagitani, Effects of phospholipids on the in vitro percutaneous penetration of prednisolone and analysis of mechanism by using attenuated total reflectance Fourier transform infrared spectroscopy, J. Pharm. Sci. 85 (1996) 1220–1226.
[24] Y. Yokomizo, H. Sagitani, Effects of phospholipids on the percutaneous penetration of indomethacin through the dorsal skin of guinea pigs in vitro, J. Control. Release 38 (1996) 267–274.
[25] G.M.M. El Maghraby, A.C. Williams, B.W. Barry, Skin delivery of oestradiol from deformable and traditional liposomes: mechanistic studies, J. Pharm. Pharmacol. 51 (1999) 1123–1134.
[26] M. McVean, D.C. Liebler, Prevention of DNA photodamage by vitamin E compounds and sunscreens: roles of ultraviolet absorbance and cellular uptake, Mol. Carcinog. 24 (1999) 169–176.
[27] E.S. Krol, K.A. Kramer-Stickland, D.C. Liebler, Photoprotective actions of topically applied vitamin E, Drug Metab. Rev. 32 (2000) 413–420.
[28] D. Luo, X.F. Lin, W. Min, Q.H. Ma, N. Gu, S.L. Jin, D.G. Wang, Photoprotection by tocopherol submicron emulsion against UV-mediated damage in HaCaT cells, Methods Find. Exp. Clin. Pharmacol. 29 (2007) 185–189.
[29] D. Darr, S. Dunston, H. Faust, S. Pinnell, Effectiveness of antioxidants (vitamin C and E) with and without sunscreens as topical photoprotectants, Acta Derm. Venereol. 76 (1996) 264–268.
[30] Y.S. Nam, J.W. Kim, J. Shim, S.H. Han, H.K. Kim, Silicone oil emulsions stabilized by semi-solid nanostructures entrapped at the interface, J. Colloid Interface Sci. 351 (2010) 102–107.
[31] Y.S. Nam, J.W. Kim, J. Shim, S.H. Han, H.K. Kim, Nanosized emulsions stabilized by semisolid polymer interphase, Langmuir 26 (2010) 13038–13043.
[32] S.S. Kwon, Y.S. Nam, J.S. Lee, B.S. Ku, S.H. Han, J.Y. Lee, I.S. Chang, Preparation and characterization of coenzyme Q(10)-loaded PMMA nanoparticles by a new emulsification process based on microfluidization, Colloids Surf. A Physicochem. Eng. Aspects 210 (2002) 95–104.
[33] H.S. Kang, J.E. Park, Y.J. Lee, I.S. Chang, Y.I. Chung, G. Tae, Preparation of liposomes containing oleanolic acid via micelle-to-vesicle transition, J. Nanosci. Nanotechnol. 7 (2007) 3944–3948.
[34] M. Rangarajan, J.L. Zatz, Effect of formulation on the delivery and metabolism of alpha-tocopheryl acetate, J. Cosmet. Sci. 52 (2001) 225–236.
[35] S.L. Banks, R.R. Pinninti, H.S. Gill, K.S. Paudel, P.A. Crooks, N.K. Brogden, M.R. Prausnitz, A.L. Stinchcomb, Transdermal delivery of naltrexol and skin permeability lifetime after microneedle treatment in hairless guinea pigs, J. Pharm. Sci. 99 (2010) 3072–3080.
[36] S. Kumar, H. Char, S. Patel, D. Piemontese, K. Iqbal, A.W. Malick, E. Neugroschel, C.R. Behl, Effect of iontophoresis on in vitro skin permeation of an analogue of growth hormone releasing factor in the hairless guinea pig model, J. Pharm. Sci. 81 (1992) 635–639.